Magnetic irreversibilities of Co/Cu/Co structures with strong antiferromagnetic exchange coupling

N. Persat
IPCMS-GEMM, CNRS-UMR 7505, ULP-ECPM, 23 rue du Loess, F-67037 Strasbourg, France and Siemens AG, ZT MF 1, Paul Gossen Strasse 100, D-91052 Erlangen, Germany

H. A. M. van den Berg
Siemens AG, ZT MF 1, Paul Gossen Strasse 100, D-91052 Erlangen, Germany

A. Dinia
IPCMS-GEMM, CNRS-UMR 7505, ULP-ECPM, 23 rue du Loess, F-67037 Strasbourg, France
(Received 6 August 1999; revised manuscript received 21 March 2000)

The irreversibilities in antiferromagnetically coupled Co/Cu/Co sandwiches prepared by dc-magnetron sputtering are shown to strongly depend on the magnetic history of the samples. The irreversibilities, evidenced by the analysis of the giant magnetoresistance and magnetization response along minor loops, are attributed to domain-phase transformations. A method is given for estimating the amount of remanence in the Co/Cu/Co sandwich, based on the analysis of the giant magnetoresistive response. The perfect antiferromagnetic alignment at zero field is attributed to the formation of a magnetic state with relative large domains. The small amount of remanence detected in some samples is ascribed to the persistence at zero field of a significant density of domain walls.

I. INTRODUCTION

The hard-soft systems[1–3] represent a wide category among the magnetic-field sensors based on the giant magnetoresistive effect (GMR). The recently introduced GMR sensor scheme[3] with the so-called artificial antiferromagnetic subsystem (AAF) offers both rigidity of the hard layers and operational temperatures up to 150° C. In its basic configuration, schematically shown in the inset of the Fig. 1, the sensor contains two antiferromagnetically coupled layers and one decoupled soft detection layer.

The Co-Cu systems are widely used in GMR sensors because of their high magnetoresistive level. Sensors containing the AAF require perfect antiferromagnetic (AF) alignment of the magnetizations right from the first Cu layer in the stack. However, the observation of incomplete AF alignment in the Co-Cu system has often been reported.[4–8] Bridges leading to direct coupling between the magnetic layers or roughness producing fluctuations between AF and ferromagnetic coupling are often mentioned to be responsible for it. The defects are attributed to the non-layer-by-layer growth mode of Co over Cu.[9,10] Complete AF alignment can nevertheless be achieved by better control of the growth parameters, or by using a surfactant.[11,12] Recently, we demonstrated that the use of an adequate buffer stack[13] leads to a negligible amount of remanence.

The knowledge of the magnetic microstructure, when aiming at producing stable sensors, is of great importance. Many techniques, like Kerr microscopy,[14] Lorentz transmission electron microscopy,[15,16] the Bitter pattern technique,[17,18] and polarized neutron reflectivity,[19] enable the observation of the domains or domain-walls in GMR systems. Barkhausen noise measurements[20] have shown in Co-Cu multilayers that the domains are relatively small when reducing the field from saturation, while they grow after reversing the field direction.

In this paper, we report on irreversible domain-phase transformations in AF coupled polycrystalline Co/Cu/Co sandwiches at the first peak in the coupling oscillation. After a brief description of the preparation, the main structural characteristics of the samples are presented. Then, we detail how the soft detection layer located in the buffer stack can be

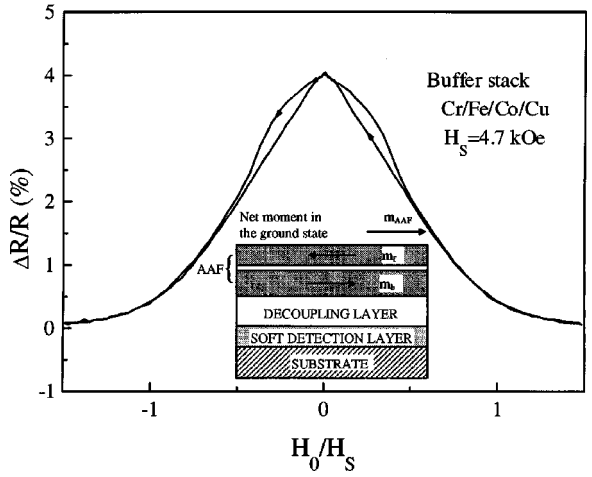

FIG. 1. The magnetoresistance curve at room temperature of the AAF Co(1.2 nm)/Cu(0.83 nm)/Co(1.2 nm) deposited on the following buffer Cr(4 nm)/Fe(1.5 nm)/Co(0.8 nm)/Cu(10 nm). The applied field H_0 is normalized to the saturation field H_S, defined as the field at which the magnetoresistance has dropped by 90%. The inset shows the basic configuration of a sensor. m_b and m_f are the moments in the so-called bias and flux conducting layers, respectively. The arrow m_{AAF} shows the direction of the AAF's net moment in the case of $m_b > m_f$.

used as a tool to judge the quality of the AF coupling. Various causes of remanence are discussed in the next section, focused on irreversible magnetic transformations.

II. SAMPLE PREPARATION AND MEASUREMENTS

The Co/Cu/Co structures presented here were prepared by sputtering on glass or on $Si/(0.5\ \mu m)SiO_2$ substrates. All samples were protected against oxidization by a Cu(2 nm)/Cr(2 nm) capping bilayer. The details on the preparation have been previously reported.[13] The buffer consists of the following stack: Cr(4 nm)/Fe(1.5 nm)/Co(0.8 nm)/Cu(10 nm). The role of the 10-nm-thick Cu layer is to smoothen the buffer and to decouple the soft magnetic layer. In AAF-based sensors, the latter is used as a soft detection layer,[3] as shown in Fig. 1.

The magnetoresistance measurements were performed at room temperature by the standard four-point method, with the sensing current perpendicular to the applied field. The magnetization curves were measured by a vibrating sample magnetometer or an alternative gradient field magnetometer at room temperature. No dead layer could be detected in single Co layers embedded in Cu layers and the Co saturation magnetization reaches 1346 ± 10 emu/cm^3, which is close to the value in bulk fcc Co (1449 emu/cm^3).

III. STRUCTURAL CHARACTERISTICS

Both the structural quality of the layers and morphology of the interfaces are decisive to obtain an AF coupling free of defects. High-angle x-ray diffraction on Co/Cu structures deposited on the Cr(4 nm)/Fe(1.5 nm)/Co(0.8 nm)/Cu(10 nm) buffer indicates that the Cr and Fe layers grow mainly in the bcc (110) direction, while the Co and Cu layers are mainly fcc (111) textured. The stabilization of the (110)-oriented Fe grains is clearly favored by the Cr seed layer. The (110) texture is of particularly great advantage when Fe is implemented in a magnetic sensor and serves as a soft detection layer, since the coercive field is appreciably reduced.

Transmission electron microscopy has been performed on samples containing an AAF and have shown that the individual layers are continuous, with flat interfaces.

Atomic force microscopy measurement was performed *ex situ*. The typical rms roughness is of the order of 0.3 nm.

The structural properties of our samples are very satisfactory and constitute an excellent basis for the occurrence of an exchange coupling free of defects.

IV. COUPLING QUALITY

As indicators for the quality of the AF coupling, we consider its strength, its completeness and its distribution.[7] These properties are closely related to the structural quality of the layers and interfaces.

A. Buffer layers

A $\approx$6-nm Fe layer is adequate for growing Co/Cu multilayers with excellent magnetoresistive properties.[6,21] Nevertheless, because of the magnetic contribution of Fe, the estimation of the amount of remanent magnetization in the Co/Cu system itself is made difficult, especially in the case of a Co/Cu/Co sandwich with thin Co layers. Although the magnetic signal of the Fe layer can in principle be easily evaluated separately, difficulties are encountered when subtracting from the total magnetization the signal of the separately grown Fe layer. This arises from the fact that the signal of this layer, in particular its coercivity, is affected by the stack grown on top.

Therefore, attempts have been made to grow Co(1.2 nm)/Cu/Co(1.2 nm) sandwiches at the first AF maximum in the coupling oscillation on nonmagnetic buffer layers. Pure Cu buffer layers ($\approx$6 nm) are hardly suited for AF coupling without coupling defects.[21] Notwithstanding significant improvement when the sandwich is deposited on a $\approx$30-nm-thick Cu layer, the remanent magnetization still reaches one-third of the saturation magnetization. Although Cr exhibits many crystallographic similarities to Fe, a pure 6-nm Cr buffer layer causes the AF coupling between the Co layers to vanish completely, even when a relatively thick (10-nm) Cu layer is put on top. This may be due to very strong surface roughness. To smoothen the surface of the Cr layer, chosen to be 4 nm thick, we cover it with a 1.5-nm Fe layer. We added a thin 0.8-nm Co to enhance the GMR signal. Finally, a 10-nm thick Cu layer is deposited, which acts as an exchange decoupling layer between the buffer stack and the Co/Cu/Co sandwich, referred as the AAF. Thus, we obtain an AAF with very satisfactory magnetoresistive properties (Fig. 1). The AF coupling strength J_{AF} reaches 0.40 erg/cm^2 at room temperature. As far as Co/Cu/Co sputtered sandwiches are concerned, J_{AF} is remarkably great, indicating the high structural quality of the layers.

B. Completeness of the coupling

In the case of sandwiches with thin magnetic layers, it is still difficult to judge from the magnetization curves whether the observed remanence is caused by the contribution of the magnetic layer in the buffer stack only. Let us now describe how this soft magnetic layer influences the magnetoresistive measurements and how the remanence of the AAF can be deduced from the magnetoresistance curve.

It is known elsewhere that the total GMR signal of the stack is well approximated by a superposition of the AAF signal and the signal due to the interaction of the AAF with the detection layer.[13]

First we shall consider the behavior of an ideal isolated AF coupled system after saturation in the positive direction. Upon reducing H_0, the moments m_1 and m_2 of the two magnetic layers (with the same modulus m) make an angle φ_1 and φ_2, respectively, with the positive direction, as indicated in the top of Fig. 2. The angles φ_1 and φ_2 have the same absolute value φ, which increases continuously between 0° and 90° as H_0 is reduced from H_S to 0. The angle φ satisfies $\cos\varphi = H_0/H_S$ for $H_0 < H_S$, and the component of the isolated AAF's moment in the positive direction satisfies $2mH_0/H_S$, as represented by the full line in Fig. 2(a). It is well established[22] that the $R(H_0)$ characteristic for perfectly AF coupled layers is quadratic, so that the normalized GMR signal of the AAF is the parabola $\Delta R_{AAF}(H_0) = 1 - \cos^2\varphi = 1 - (H_0/H_S)^2$ [the full line in Fig. 2(b). Let us now consider the interaction between the AF coupled system and the magnetic layer of the buffer stack with moment m_D, supposed to

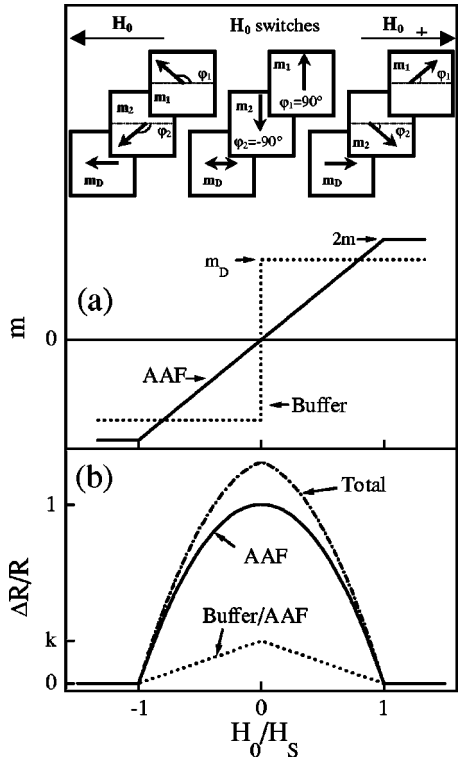

FIG. 2. Stylized $m(H_0)$ and $\Delta R/R(H_0)$ curves. In (a), the full line corresponds to the response of the isolated AF coupled system and the dotted line to the soft magnetic layer. In (b), the full line is $\Delta R_{\mathrm{AAF}}(H_0)$, the dotted line is $\Delta R_{\mathrm{INT}}(H_0)$ and the dotted dashed line is their superposition. In the top, m_1 and m_2 represent the moments within the AF coupled system and m_D the moment in the soft magnetic layer. Note the perpendicular orientation of the magnetizations within the AAF at zero field, relative to the positive direction.

have an ideal soft-magnetic stepwise response [the dotted line in Fig. 2(a)]. As H_0 is reduced from H_S to 0, m_D remains aligned in the positive direction, so that the absolute value of the angle between m_D and m_1 (m_2) is φ. The GMR signal resulting form this interaction is known[22] to vary linearly with $\cos\varphi$. Therefore, the GMR signal resulting from this interaction is roughly given by $\Delta R_{\mathrm{INT}}(H_0)=k(1-H_0/H_S)$ for $H_0<H_S$ [the dotted line in Fig. 2(b)], where k is the ratio of the level of this interaction to the level of the signal of the AAF and corresponds to the rotation of the detection layer from 0° to 90°, and adds to $\Delta R_{\mathrm{AAF}}(H_0)$, so that the total GMR signal is modified [the dotted-dashed line in Fig. 2(b)]. The slope of this curve at $H_0=0$ is related to the magnitude of $\Delta R_{\mathrm{INT}}(H_0)$. This simple model applies well if one considers the upper branches of the magnetoresistance curve of Fig. 1.

Let us now consider the case of a small lag $\Delta\varphi$ in the magnetic response of the AAF. Such a $\Delta\varphi$ can be represented by ΔH, being the additional field, to compensate for this lag. A problem arises when the remanence of the AAF to be determined from the transport curves, because of the parabolic shape, i.e., the zero slope of that curve at the origin. As we know from the $\Delta R_{\mathrm{INT}}(H_0)$ interaction, the slope of this interaction is much higher and the remanence of the AAF can easily be determined.

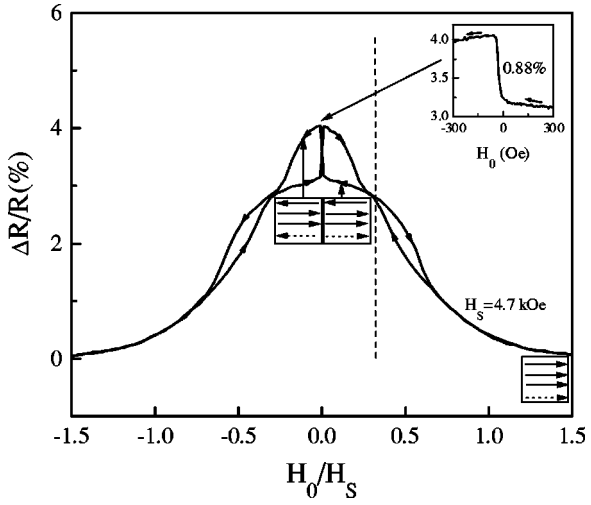

FIG. 3. The magnetoresistance curve at room temperature of the AAF Co(1 nm)/Cu(0.5 nm)/Co(1 nm)/Cu(0.83 nm)/Co(1 nm) deposited on the Cr(4 nm)/Fe(1.5 nm)/Co(0.8 nm)/Cu(10 nm) buffer. The arrows in the boxes represent the magnetic moments as a function of the field. The dashed arrow corresponds to the soft magnetic layer's moment, and the full arrows to the moments of the Co layers in the AAF. The inset details the GMR response upon switching of the soft detection layer in the buffer stack. Glass substrates are used.

C. The maximum signal of the detection layers

The question of the determination of the maximum possible jump on the GMR upon switching of the soft detection layer is in order. This maximum jump would be detected if m_1 and m_2 would be ''pinned'' in the positive direction at $H_0=0$. In this case, upon switching of H_0, the change of angle between m_D and m_1 (m_2) would be of 180°, giving rise to a jump of $2k$ on the GMR. This is twice the level k of the interaction between the perfect AAF and m_D represented in Fig. 2(b), since there, the relative angle varied continuously between 0° and 90° only. To obtain the desired fixation of m_1 and m_2 in the positive direction, the following layer sequence is prepared: Co(1 nm)/Cu(0.5 nm)/Co(1 nm)/Cu(0.83 nm)/Co(1 nm). The Cu(0.5 nm) layers couples ferromagnetically the two first Co layers in order to attach m_1 and m_2 together. The second Cu(0.83 nm) layer ensures AF coupling between this pair and the third Co layer in order to ''pin'' the pair in the positive direction. The total friction against rotation of the subsystem's magnetization is increased[3] by about a factor of 3 compared to a single magnetic layer with the same total Co thickness (3 nm). It is essential to note that in the ground state at zero field, the magnetic moments of the first pair are antiparallel aligned to the third Co layer and lie in the positive direction. This is schematically represented by the arrows in Fig. 3. The extra magnetic layer does not significantly contribute to the GMR interaction with the detection layer, so that the maximum jump at zero field, $2k$, will be approximately reproduced.

A plateau in the magnetization curve, and consequently in the GMR curve, corresponding to the regime with opposite alignment of the moments is predicted[3] at $H_P=H_S/3$. It is clearly recognized in Fig. 3, which presents the GMR signal as a function of the normalized field H_0/H_S for the Co(1

nm)/Cu(0.5 nm)/Co(1 nm)/Cu(0.83 nm)/Co(1 nm) sandwich. The dashed vertical line at $H_0/H_S = 1/3$ corresponds well to the occurrence of the plateau.

We have argued in Sec. IV B that a small stepwise increase in the GMR signal is expected to occur upon switching of the soft-magnetic layer when an AF coupled symmetrical sandwich shows remanence. In the specially designed subsystem presented just above, the jump detected around zero field roughly is the GMR increase (0.88%) that would be observed if the sandwich had 100% remanence. Assuming that steps of 0.025% can easily be detected in the magnetoresistance curves, this means that a relative remanence of 3% in an AAF coupled system can be easily recognized in the GMR signal. Therefore, GMR response is a very interesting tool for estimating a small amount of remanence in coupled sandwiches.

V. IRREVERSIBLE TRANSITIONS

The GMR curves presented in Sec. IV all exhibit a clear hysteretic behavior. To clarify the origin of the differences between the branches, the magnetoresistance and the magnetization have been measured along minor loops. The minor loops start at positive saturation, then the applied field H_0 is reduced to a minimum value H_{rev}, being either positive or negative, and finally, H_0 is increased again toward positive saturation. The major loop corresponds to a complete hysteresis cycle.

A. Positive reversal field H_{rev}

Five minor loops with H_{rev} values between 713 Oe and 1.21 kOe are presented in Fig. 4(a). The minor loops with $H_{\mathrm{rev}} = 1.21$ kOe and $H_{\mathrm{rev}} = 1.06$ kOe are fully reversible, as recognized by the fact that both their $R(H_0)$ branches coincide with the lower $R(H_0)$ branch of the major loop. For $H_{\mathrm{rev}} = 962$ Oe, an irreversible process starts to occur: the return branch (i.e., increasing applied field) starts to split up from the one with the lowest $R(H_0)$ values. This means that 962 Oe is just below the threshold value H_{T1} at which irreversible changes start to take place. Upon further reducing H_{rev} well below H_{T1}, the irreversibility becomes more and more pronounced, as for with $H_{\mathrm{rev}} = 894$ Oe and $H_{\mathrm{rev}} = 713$ Oe in Fig. 4(a).

The magnetization of this sample has been measured along five minor loops as shown in Fig. 4(b). The major loop also presents hysteretic behavior. The branch with the highest mean magnetization $M(H_0)$ along the applied field forms the pendant to the branch of the GMR curve with the lowest $R(H_0)$ signal, while the branch with the lowest $M(H_0)$ is the counterpart of the GMR branch with the highest $R(H_0)$. The minor loops with $H_{\mathrm{rev}} > 926$ Oe are fully reversible. Below the transition field value $H_{\mathrm{T1}} = 926$ Oe, the irreversibility occurs and becomes more visible for $H_{\mathrm{rev}} = 821$ Oe and $H_{\mathrm{rev}} = 622$ Oe.

The values of the transition field H_{T1} found by GMR and AGFM measurements are in good agreement, and the small subsisting discrepancy can be attributed to the sensitivity of the detection method.

Now we shall delve deeper into the origin of the observed irreversibility. Since no effective anisotropy is present in our

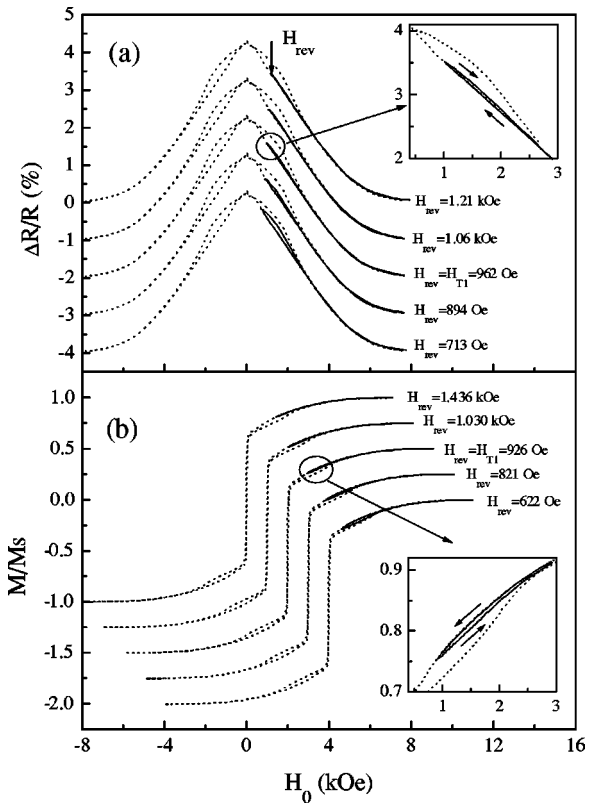

FIG. 4. The (a) magnetoresistance and (b) magnetization minor loops with positive values of H_{rev} for the AAF Co(1.2 nm)/Cu(0.83 nm)/Co(1.2 nm) sandwich. Each of the minor loops is superposed for comparison on the major loop. The inset details in each case the irreversibility due to domain-phase transformations at the field H_{T1}. In (a) the vertical scale is common to all curves, shifted by 1% for clarity. In (b) both vertical and horizontal scales are common, shifted by 0.5 and 1 kOe respectively, for clarity.

systems, we expect that the irreversibility in the GMR and $M(H_0)$ signals, in the present structure, can be attributed to a domain-phase transformation process. The domain configuration develops when leaving the parallel state at saturation. Ideally, the magnetization inside each Co layer would start to rotate uniformly and reach the perfect AF alignment at zero field, with both magnetizations perpendicular to the original saturation field [see m_1 and m_2 in Figure 2(a)]. The polycrystalline character of our Co layers originates in the amorphous nature of the SiO_2 substrate. As a consequence, there is no macroscopic anisotropy and no unique sense of the rotation of the magnetization in a given layer is imposed. Therefore, half of the moments inside the crystallites will rotate clockwise and half will rotate counterclockwise in a specific layer. This results in the formation of magnetic domain structures. Inhomogeneities may add to the thermal activation and facilitate the local rotation of the moments. For example, stepwise variations in the spacer thickness produce inhomogeneities in the coupling distribution so that the rotation starts at different fields at different positions. This hinders a rotation in unison of the layer's magnetization. Upon reducing H_0, the moments inside the areas presenting the strongest coupling should rotate first. Upon reducing further H_0, the magnetization inside the areas with weaker AF coupling also rotate. Here, the sense of the rotation may be im-

posed by neighboring regions in which the sense of the rotation is already established. Finally, more and more moments rotate and domain walls with Néel-type of structure are created when domains with different sense of rotation of the magnetization in a given Co layer meet.

We will now return to the domain conversion process. As long as the wall angles are small enough, the configuration with a high density of domains remains stable and the wall angles can vary in a reversible fashion. This is the case of the fully reversible minor loops of Figs. 4(a) and 4(b). Upon reducing H_0 below a certain threshold value, the presence of domain walls becomes unfavorable. As a consequence, domains will annihilate and cause the separation of the descending and ascending field branches in Figs. 4(a) and 4(b). A further reduction of H_0 makes more and more domains vanish. Finally, the return path of the minor loop reaches the highest branch of the major GMR curve (or the lowest branch of the magnetization curve). This branch is characterized by a low density of domains.

B. Negative reversal field H_{rev}

At zero field after positive saturation, we arrive at a similar state with low density of walls. However, the magnetization in the adjacent layers are opposite now. Let us now look at the transformations arising from the antiparallel state by considering the minor loops with H_{rev} taking negative values. Figure 5(a) presents the GMR signal of the AAF measured along five such loops. The minor loops with $H_{rev} > -1.910$ kOe are fully reversible. The irreversibility is visible at $H_{rev} = -1.910$ kOe and becomes more pronounced for $H_{rev} = -2.010$ kOe and $H_{rev} = -2.211$ kOe. The same phenomenon is reflected in the five magnetization minor loops of Fig. 5(b), with the same value of the threshold field, H_{T2}.

Upon increasing the applied field in the negative direction from the AF state, the magnetization inside the large domains is forced to rotate to reach the parallel alignment. As long as no regions have reached this state, no new domains are formed upon a subsequent reduction of the field to zero, because the sense of the rotation to the antiparallel alignment is already defined. The magnetic phase with low domain density is maintained and it is possible to move in a reversible way along the upper branch of the GMR curve (or along the lowest branch of the magnetization curve). However, as soon as areas with the weakest AF coupling are saturated, domains are likely to be created again upon reducing the strength of the field due to the freedom in the sense of the rotation, as discussed in Sec. V A for the descending field flank. For larger H_{rev} absolute values, more and more regions are ferromagnetically aligned, according to the interlayer coupling distribution, so that more and more domains are created at the return path.

VI. CONCLUSION

We have studied the domain-phase transformations occurring in AF coupled sandwiches. Buffer stacks containing the Cr/Fe bilayer are very well suited for depositing high-quality samples with (111) texture of the sputtered Co-Cu layers. A method was presented that allows us to judge the completeness of the AF coupling in sandwiches by the height of the jump in the GMR response that occurs upon switching the soft magnetic layer. It is possible to obtain Co/Cu/Co sandwiches at the first maximum in the coupling oscillation without detectable remanence by use of an adequate buffer, as verified by stack containing asymmetrical AAF. The residual remanence is possibly related to the presence of domain walls at zero field. Domains are created upon reducing the field from the saturated state, due to the freedom in the sense of the magnetization's rotation. The irreversibilities observed in GMR and magnetization curves are attributed to domain-phase conversion. In cases with zero remanence, the annihilation is complete.

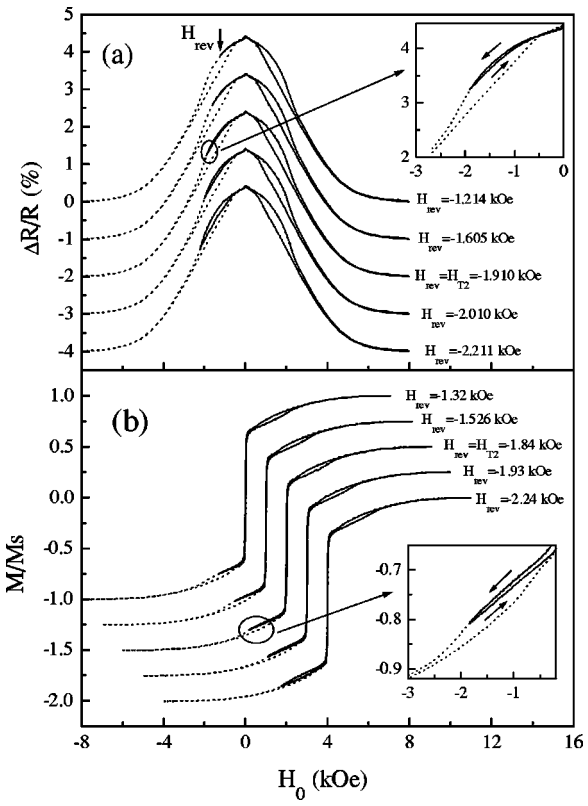

FIG. 5. The (a) magnetoresistance and (b) magnetization minor loops with negative values of H_{rev} for the AAF Co(1.2 nm)/Cu(0.83 nm)/Co(1.2 nm) sandwich. Each of the minor loops is superposed for comparison on the major loop. The inset details in each case the irreversibility due to domain-phase transformations occurring at the field H_{T2}. In (a) the vertical scale is common to all curves, shifted by 1% for clarity. In (b) both vertical and horizontal scales are common, shifted by 0.5 and 1 kOe respectively, for clarity.

ACKNOWLEDGMENTS

This work was partly supported by the Brite Euram ''Contactless position sensors based on new GMR multilayer materials.'' We thank our colleagues from Siemens and IPCMS for technical assistance and fruitful discussions: G. Gieres, K. H. Rojek, H. Mai for the samples preparation, G. Rupp for magnetotransport measurements, K. Cherifi-Khodjaoui for x-ray diffraction, H. Cerva for TEM, M. Demand and C. Tiusan for AFM measurement, and D. Stoeffler for fruitful discussions.

[1] R. Kergoat, J. Miltat, T. Valet, and R. Jérome, J. Appl. Phys. **76**, 7087 (1994).
[2] B. Dieny, V.S. Speriosu, S.S.P. Parkin, B.A. Gurney, D.R. Wilhoit, and D. Mauri, Phys. Rev. B **43**, 1297 (1991).
[3] H.A.M. van den Berg, W. Clemens, G. Gieres, G. Rupp, W. Schelter, and M. Vieth, IEEE Trans. Magn. **32**, 4624 (1996); H.A.M. van den Berg, W. Clemens, G. Gieres, G. Rupp, M. Vieth, J. Wecker, and S. Zoll, J. Magn. Magn. Mater. **165**, 524 (1997); W. Clemens, H.A.M. van den Berg, G. Rupp, W. Schelter, M. Vieth, and J. Wecker, J. Appl. Phys. **81**, 4310 (1997).
[4] R.J. Highmore, W.C. Shih, R.E. Somekh, and J.E. Evetts, J. Magn. Magn. Mater. **116**, 249 (1992).
[5] A. Schreyer, K. Bröhl, J.F. Ankner, C.F. Majkrzak, Th. Zeidler, P. Bödeker, N. Metoki, and H. Zabel, Phys. Rev. B **47**, 15 334 (1993).
[6] G. Rupp and K. Schuster, J. Magn. Magn. Mater. **121**, 416 (1993); G. Rupp and H.A.M. van den Berg, IEEE Trans. Magn. **29**, 3102 (1993); H.A.M. van den Berg and G. Rupp, *ibid.* **30**, 809 (1994).
[7] H.A.M. van den Berg and S. Schmeusser, IEEE Trans. Magn. **29**, 3099 (1993); H.A.M. van den Berg, in *Magnetic Thin Films and Multilayer Systems: Physics, Analysis and Industrial Applications*, edited by U. Hartmann (Springer, Berlin, 1997); H.A.M. van den Berg, J. Wecker, and H. Schewe, Current Topics Magnet. Res. **1**, 235 (1994).
[8] N. Persat, A. Dinia, J.P. Jay, C. Mény, and P. Panissod, J. Magn. Magn. Mater. **164**, 37 (1996); N. Persat and A. Dinia, Phys. Rev. B **56**, 2676 (1997).
[9] J. de la Figuera, J.E. Prieto, C. Ocal, and R. Miranda, Phys. Rev. B **47**, 13 043 (1993).
[10] R. Castañer, C. Prieto, A. de Andrés, J.L. Martínez, J. Trigo, and J.M. Sanz, Solid State Commun. **98**, 179 (1996).
[11] J. Camarero, T. Graf, J.J. de Miguel, R. Miranda, W. Kuch, M. Zharnikov, A. Dittschar, C.M. Schneider, and J. Kirschner, Phys. Rev. Lett. **76**, 4428 (1996).
[12] W.F. Egelhoff, Jr., P.J. Chen, C.J. Powell, M.D. Stiles, R.D. McMichael, C.L. Lin, J.M. Sivertsen, J.H. Judy, K. Takano, A.E. Berkowitz, J. Appl. Phys. **80**, 5183 (1996).
[13] N. Persat, H.A.M. van den Berg, and A. Dinia, J. Magn. Magn. Mater. **165**, 446 (1997); N. Persat, H.A.M. van den Berg, K. Cherifi-Khodjaoui, and A. Dinia, J. Appl. Phys. **81**, 4748 (1997).
[14] R. Schäfer, A. Hubert, and S.S.P. Parkin, IEEE Trans. Magn. **29**, 2738 (1993).
[15] L.J. Heyderman, J.N. Chapman, and S.S.P. Parkin, J. Appl. Phys. **76**, 6613 (1994).
[16] T. Zimmerman, J. Zweck, and H. Hoffmann, J. Magn. Magn. Mater. **149**, 409 (1995).
[17] M.A.M. Gijs, J.B. Giesbers, P. Beliën, J.W. van Est, J. Briaire, and L.K.J. Vandamme, J. Magn. Magn. Mater. **165**, 360 (1997).
[18] S.Z. Hua, D.S. Lashmore, L.J. Swartzendruber, W.F. Egelhoff, Jr., K. Raj, and H.D. Chopra, J. Appl. Phys. **81**, 4582 (1997).
[19] J.A. Borchers, P.M. Gehring, R.W. Erwin, J.F. Ankner, C.F. Majkrzak, T.L. Hylton, K.R. Coffey, M.A. Coffey, M.A. Parker, and J.K. Howard, Phys. Rev. B **54**, 9870 (1996).
[20] H.T. Hardner, M.B. Weissman, M.B. Salamon, and S.S.P. Parkin, Phys. Rev. B **48**, 16 156 (1993); H.T. Hardner, M.B. Weissman, B. Miller, R. Loloee, and S.S.P. Parkin, J. Appl. Phys. **79**, 7751 (1996).
[21] S.S.P. Parkin, R. Bhadra, and K.P. Roche, Phys. Rev. Lett. **66**, 2152 (1991).
[22] B. Dieny, J. Magn. Magn. Mater. **136**, 335 (1994).